

## Electronic properties of the narrow-band material $\alpha$ -RuCl<sub>3</sub>

I. Pollini

*Istituto Nazionale per la Fisica della Materia, Unità di Ricerca di Milano, c/o Dipartimento di Fisica, Via Celoria 16, 20133 Milano, Italy*

(Received 26 July 1995; revised manuscript received 2 January 1996)

X-ray angle-integrated and ultraviolet angle-resolved photoemission spectra of the low-spin compound  $t_{2g}^5$   $\alpha$ -RuCl<sub>3</sub> show that Ru 4*d* and Cl 3*p* states contribute to the valence-band structure of this magnetic material. The energy distribution curves measured along the azimuthal directions  $\Gamma$ -*M'*- $\Gamma$  and  $\Gamma$ -*K*-*M* using He I radiation indicate an uppermost nearly dispersionless structure of Ru 4*d* origin, and two dispersive features obtained from Cl 3*p*-derived bands. The photoemission results, together with the optical and magnetic properties described by ligand-field theory, support the view of localized 4*d* states forming a very narrow Ru 4*d* band in the vicinity of the Fermi energy. The main 4*d* emission structure has been thus assigned to 4*d*<sup>4</sup> unscreened hole states, where the band gap corresponds to intersite *d*-*d* transitions, and  $\alpha$ -RuCl<sub>3</sub> can be classified as a Mott-Hubbard compound in consideration of its electronic and magnetic characteristics. The inconsistency between the photoemission results and the transport properties, describing this material as a conventional band-gap semiconductor, is finally discussed.

### I. INTRODUCTION

The nature of the electronic structure and the origin of the insulating gap in transition-metal oxides (TMO's) and halides (TMH's) has been a controversial subject for many years.<sup>1-6</sup> One-electron band-structure calculations predict small energy gaps for TMO's,<sup>5,6</sup> and even metallic behavior both for TMO's and TMH's; like Ni dihalides and Cr trihalides.<sup>7</sup> As a matter of fact, transition-metal compounds (TMC's) reveal two different types of electronic behavior: the delocalized regime, as in layer dichalcogenides, and the localized one, with examples taken frequently from the TMO's and TMH's. The delocalized regime, which is described by the independent-electron approximation, adheres to band-structure calculations very satisfactorily to produce either metallic behavior or semiconductivity. On the other hand, localized materials show an insulating behavior, largely independent of band-structure previsions (e.g., CrCl<sub>3</sub> and Cr<sub>2</sub>O<sub>3</sub> are excellent insulators with partially filled *d* bands), with the breakdown due to the growth of electron-electron correlation to produce *d* electrons essentially trapped around each TM site. In this case the optical and magnetic properties are described by ligand-field theory.<sup>8</sup> TMH's are, in general, antiferromagnetic, electrically insulating, ionic compounds presenting layered structures (e.g., CdCl<sub>2</sub>, CdI<sub>2</sub>, and BiI<sub>3</sub>). The halide *p* bands are fully occupied, the metal *s* states are empty, and the metal *d* states are partially occupied. It is the apparent incompatibility of their insulating behavior with the partial occupation of the *d* shell that makes these materials especially interesting.<sup>1,2</sup> Although attempts at modifying band theory to explain the insulating behavior have been made, it does not appear likely that a pure Hartree-Fock (HF) approach will consistently account for the electrical behavior of all TMC's. Two approaches (band theory with exchange interaction treated in the density-functional approximation, and the local cluster model) make clear predictions concerning the structures which should be observed in direct and inverse photoemis-

sion spectroscopy as well as in optical spectroscopy. The most striking difference between the two approaches concerns the magnitude of the conductivity gap. However, as far as TMO's are concerned, it seems now more or less accepted that the  $\sim 4$ -eV gap of MnO, FeO, CoO, and NiO arises from Mott-Hubbard localization of electrons in partly filled *d* bands. Recently, it has been suggested that hybridization of the localized 3*d* levels and O 2*p* bands in some TMO's (such as NiO and CuO), and halide *p* bands in some TMH's,<sup>3,4,9</sup> is of critical importance, and that the insulating gap is actually of the charge-transfer type (CuCl<sub>2</sub>, CuBr<sub>2</sub>, and NiX<sub>2</sub>) (*X* = Cl, Br, or I). However, despite the apparent breakdown in band theory that this approach represents, one-electron models have been successful in correctly determining the lattice spacings, magnetic moments, and energy gaps, besides antiferromagnetic (AF) order.<sup>5,6,10,11</sup> Moreover, recent theoretical work<sup>5,11,12</sup> has revived the idea that the principal origin of the band gap is the inherent AF order: in this itinerant 3*d*-electron model of the TMO, the exchange perturbation of the one-electron band structure opens a *d*-*d* gap.

An explanation for this failure of band theory was first suggested by Mott,<sup>13,14</sup> who brought attention to the importance of electronic correlation, neglected in a HF approach, in the case of narrow bands: Mott pointed out that in the limit where the lattice parameter becomes sufficiently large that overlap between nearest-neighbor electronic wave functions is negligible, any material must be an insulator. In the limit of zero-width bands, electrons are localized around their ion cores, just as core electrons. The existence of a correlation gap in a simple model, consisting of a single *s* band with a  $\delta$ -function interaction between electrons, was then verified by Hubbard.<sup>15</sup>

Furthermore, TMO's and TMH's are ideal subjects for an investigation of insulating and metallic states, because of the wide diversity of electrical properties observed in apparently similar materials: for example, layered CrCl<sub>3</sub> and cubic Cr<sub>2</sub>O<sub>3</sub> are both Mott insulators, while layered RuCl<sub>3</sub> is apparently a Mott-Hubbard compound (or a not standard semi-

conductor) and cubic  $\text{RuO}_2$  a metal. A major problem for these materials is the preparation of good crystals, since most of them contain important concentrations of random impurities and lattice defects so that the results of electrical measurements often have little to do with the intrinsic properties of the material. Most pure, stoichiometric crystalline materials are classified as either metals ( $10^{-6} < \rho_{\text{RT}} < 10^{-2} \Omega \text{ cm}$ ) with a linear increase of the resistivity  $\rho$  with the temperature  $T$  or insulators and semiconductors ( $10^3 < \rho_{\text{RT}} < 10^{17} \Omega \text{ cm}$ ) and an exponential decrease with increasing temperature. Some typical insulators include  $\text{NiO}$ ,  $\text{TiO}_2$ ,  $\text{CoO}$ ,  $\text{Cr}_2\text{O}_3$ , and  $\text{CrCl}_3$ , and metals include  $\text{TiO}$ ,  $\text{CrO}_2$ ,  $\text{ReO}_3$ , and  $\text{RuO}_2$ . Charge-transfer semiconductors are  $\text{CuO}$ ,  $\text{CuCl}_2$ ,  $\text{NiCl}_2$ , and  $\text{NiBr}_2$ : holes are light (transport in the anion valence band) and electrons are heavy (transport in the  $d$  band).<sup>4,9</sup>

In a recent paper,<sup>16</sup> the core and valence-band photoemission (PE) spectra of layered  $\text{CrCl}_3$  and  $\alpha\text{-RuCl}_3$  were measured and discussed. The only difference was a larger width ( $\sim 5$  eV) of the valence band as compared to the core levels, which reflects the dispersion of the bands. These materials were classified as Mott-Hubbard (MH) insulators on the basis of experimental results obtained by angle-integrated photoemission (AIP), photoconductivity, and optical spectra. The interpretation of PE spectra becomes more complicated in compounds that contain open shell ions like transition metals, and the principal conclusions were that the  $3d$  and  $4d$  states of Cr and Ru atoms and  $3p$  states of Cl contribute to the formation of the valence band, and that the main  $d$ -band emission is due to crystal-field multiplets of the  $d^{n-1}$  final states.<sup>16,17</sup>

For MH compounds, the energy gap  $E_G$  is proportional to  $U$ , the  $d$ - $d$  Coulomb interaction which includes exchange and correlation, and both holes and electrons are heavy since they move in bands (Hubbard bands) formed primarily from  $d$  orbitals of the transition-metal ions, and these are narrow because the ions are relatively far apart. The electrostatic repulsion between the electrons leads to localization of the  $d$  electrons and a nonconducting state: two typical examples are  $\text{CrCl}_3$  (Ref. 16) and  $\text{Cr}_2\text{O}_3$ .<sup>17</sup> In a  $4d$  TM compound ( $\text{RuCl}_3$ ), the situation is rather different from a  $3d$  TM compound ( $\text{CrCl}_3$ ), since  $\text{RuCl}_3$  is in the low-spin state. The  $4d$  electrons, being less tightly bound energetically and spatially than the  $3d$  electrons, are more directly exposed to the ligands, have a greater state mixing with an increase in the crystal-field (CF) splitting parameter  $\Delta_{\text{CF}}$ , and at the same time they show a smaller value of the Racah parameter  $B$ , which gives a measure of the electron-electron repulsion within the  $d$  shell.<sup>8,18-20</sup> In Table I some examples illustrate the high-low change of these parameters.

In Ref. 16 it was anticipated that the relative dispersion of Ru  $4d$  states in the valence band would be less than 0.2 eV, on the ground of preliminary angle-resolved photoemission (ARP) measurements, and that the photoconductivity excited across the  $d$ - $d$  energy gap  $E_G$  could be due to a hopping type of conduction where the electrons diffuse from one cation site to the next.

However, this picture does not seem consistent with reported conductivity<sup>18,21</sup> and Hall mobility data<sup>21</sup> which describe this material as a traditional semiconductor ( $\rho_{\text{RT}} \sim 10^3 \Omega \text{ cm}$ ), where the intrinsic electrical transport is

TABLE I. High-low spin change of the crystal-field parameters for some  $3d$  and  $4d$  transition-metal compounds. The  $4d$  electrons present an increase in the crystal-field splitting parameter  $\Delta_{\text{CF}}$  and smaller values of the Racah parameter  $B$ , (h.s. and l.s. means high-spin and low-spin compounds, respectively). Values for  $\text{CrCl}_3$  and  $\text{RuCl}_3$  are taken from Refs. 19 and 18, respectively; those for  $\text{MoCl}_3$  and  $\text{FeCl}_3$  are from Ref. 20.

	$\Delta_{\text{CF}}$ ( $\text{cm}^{-1}$ )	$B$ ( $\text{cm}^{-1}$ )	$\Delta_{\text{CF}}/B$
$3d^3$ $\text{CrCl}_3$ h.s.	13.700	540	25.4
$4d^3$ $\text{MoCl}_3$ l.s.	19.300	410	47
$3d^5$ $\text{FeCl}_3$ h.s.	14.000	750	18.5
$4d^5$ $\text{RuCl}_3$ l.s.	11.840	370	32

due to electrons which move with a bandlike mechanism within the  $4d$  narrow CF bands with a very low mobility ( $0.1 < \mu < 1 \text{ cm}^2 \text{ V s}^{-1}$ ) and a high effective mass. The inconsistency between the photoemission results and transport properties raises the question whether  $\alpha\text{-RuCl}_3$  is a band or a Mott compound (semiconductor). This problem is not new, as some examples reported in the literature point out: see, for instance, the case of  $\text{TMO}$ ,<sup>5</sup>  $\text{CoO}$ ,<sup>22</sup> and  $\text{TiTe}_2$ .<sup>23</sup>

In seeking a means of clarifying this point, it seems natural to turn to photoemission techniques, since they have played a major role in testing the electronic structure of a wide variety of materials, including oxides. In principle, ARP should be able to distinguish between localized and itinerant (bandlike)  $d$  states by the observation (or not) of the energy peak dispersion with the electron wave vector.

Hence the results of an ARP study are presented and discussed in relation to the known electronic and transport properties. Further, some considerations concerning the metallic and insulating behavior of  $\text{RuO}_2$  (Refs. 24–28) and  $\text{RuCl}_3$  materials, where the electrical transport may or not occur in partially filled  $d$  bands, are made by discussing their x-ray photoemission spectra (XPS).

## II. SAMPLE PREPARATION AND EXPERIMENTAL PROCEDURE

Crystals of  $\alpha\text{-RuCl}_3$  were grown from the vapor phase by chemical transport in an open tube reactor. The metal powder reacts at approximately  $750^\circ \text{C}$  with a stream of  $\text{Cl}_2$  gas, and crystals are deposited at lower temperature in the growth zone. The purity of the elements (Ru metal powder and  $\text{Cl}_2$  gas) is greater than 99.9%, and  $\text{RuCl}_3$  crystals may present a stoichiometry deviation around 1%, as measured for the pure compounds. This slight deviation of stoichiometry is too small to be discernable in the photoemission spectra, but can affect the electrical measurements, owing to their sensitivity to lattice defects and impurities. The crystals ( $\sim 25 \text{ mm}^2$ ) are black, lustrous, and very stable with thickness between 10 and  $70 \mu\text{m}$ .

$\alpha\text{-RuCl}_3$  has the high-temperature crystal structure of  $\text{CrCl}_3$  ( $C_{2h}^3$  monoclinic, four formula units per unit cell above  $240 \text{ K}$ ). It belongs to a group of layered transition metal halides where one hexagonal sheet of atoms (Ru) is sandwiched between two hexagonal sheets of chlorine. However, for  $\text{RuCl}_3$  two-thirds of the Ru atoms are missing in the metallic sheet, and the structure of the surface of  $\text{RuCl}_3$  is

identical to that of  $\text{BiI}_3$ . Within a sandwich the bonding is mainly of ionic character (the coordination around the metal atom is octahedral), whereas the van der Waals bonding is responsible for the stacking between the sandwiches.  $\alpha\text{-RuCl}_3$  is antiferromagnetic below 13 K.<sup>16</sup> The rhombohedral unit cell consists of two metal and six halogen atoms. The three-dimensional Brillouin zone (BZ), and its related surface BZ is identical to that of  $\text{CdCl}_2$ -type compounds. The  $M$  and  $M'$  surface symmetry points correspond to inequivalent directions when the underlying structure is taken into account. The surface Brillouin zone arises from the halogen atoms, which are 0.36 nm distant from each other: it follows that  $\Gamma K = 12.8 \text{ nm}^{-1}$  and  $\Gamma M = 11.1 \text{ nm}^{-1}$ .

Owing to the surface sensitivity of ultraviolet-photoelectron spectroscopy (UPS) photoemission, the samples were peeled in the  $10^{-8}$ -Pa range, and the quality of the basal plane was controlled by low-energy electron diffraction (LEED). Since the LEED diagrams do not discriminate between  $M$  and  $M'$ , a careful examination was made of the absolute PE intensity vs the polar angle in order to specify the different crystallographic orientations. The  $\Gamma M$  and  $\Gamma M'$  directions were identified as follows: going from a metal atom along the  $\Gamma M$  direction the first-neighbor ligand lies under the  $\Gamma M$  line, whereas in the  $\Gamma M'$  direction it lies above the  $\Gamma M'$  line.

XPS experiments were performed with a Vacuum Generators ESCALAB MKII system, equipped with a monochromatized Al  $K\alpha$  x-ray source ( $\hbar\omega = 1486.6 \text{ eV}$ ): the angular acceptance of photoelectrons is so large that in the final state the wave vector  $k$  of the photoelectrons is smeared out over a large part of the whole BZ. There is a second effect: for electromagnetic radiation of 1.5 keV, the photon wave vector is relatively large,  $\kappa \approx 0.7 \text{ \AA}^{-1}$ , and therefore one no longer has a vertical transition. This adds to averaging over the BZ. In experiments using a polycrystalline sample, the XPS spectrum, therefore, reproduces the density of states (DOS) of the material, in which contributions from electrons with different angular momenta are weighted differently because of their different photoelectric cross sections. In experiments with single crystals, this XPS density of states is further modulated with an angular projection factor. However, although experience has shown that, in general, single-crystal experiments on pure materials do not give much more detailed information than experiments with polycrystalline samples, in the case of  $\text{RuCl}_3$  XPS spectra measured on single crystals have exhibited a structure unnoticed in previous works.<sup>16</sup> The total instrumental resolution was about 1 eV.

In the UPS (ultraviolet photoelectron spectroscopy) regime, the spectra are dominated by direct (vertical) transitions in the reduced zone scheme. In an experiment with a single-crystal sample, one investigates direct transitions with well-defined  $k$  vectors. This then provides a method to map the band structure  $E(k)$ . The spectra were obtained in an ultrahigh vacuum system ( $10^{-10}$ -mbar range) with an hemispherical energy analyzer by using a He discharge lamp (He I,  $\hbar\omega = 21.2 \text{ eV}$ ). The photon beam had an incidence angle  $\alpha_i = 45^\circ$  with respect to the normal at the sample surface. The energy resolution was about 150 meV, and the acceptance angle was  $\pm 1^\circ$ . The polar angle  $\theta$  of emission was incremented by  $5^\circ$  steps from  $0^\circ$  to  $80^\circ$ . The energy

distribution curves were measured along different azimuthal directions  $\Gamma M$ ,  $\Gamma M'$ , and  $\Gamma K$  in the BZ.

The polar angle dependence of the spectra for the  $\Gamma M'$  and  $\Gamma K$  directions has been measured with a normalized photoemission intensity, and we have calculated the  $k_{\parallel}$  values associated with the peak positions on the photoemission spectra using the equation

$$k_{\parallel} = \left( \frac{2mE_k}{\hbar^2} \right)^{1/2} \sin\theta, \quad (1)$$

with  $E_k = \hbar\omega - W - E_i$ , where  $E_k$  is the kinetic energy of the photoelectrons,  $W$  the work function,  $\hbar\omega$  the photon energy, and  $E_i$  the energy of the initial state of the transition. The position of the Fermi level ( $E_F$ ) was determined from the photoelectron spectrum of gold evaporated on the sample, as a reference metal. The work function was obtained by subtracting the width of the photoelectron energy distribution (from zero kinetic energy to  $E_F$ ) from the radiation energy: the vacuum level was so found at 6.1 eV above the Fermi level.

### III. RESULTS AND DISCUSSION

Figure 1 presents the UPS and XPS valence-band spectra of  $\alpha\text{-RuCl}_3$ , and the XPS spectrum of the metallic compound  $\text{RuO}_2$  ( $4d^4$ ). The PE spectra of  $\text{RuCl}_3$  are formed by three resolved bands originating from the Ru  $4d$  and Cl  $3p$  states: the metal  $4d$  band and Cl  $3p$  bands are still separated, although some metal-chlorine hybridization is present. The symmetry attributions follow from the strong increase of the photoemission intensity from the Ru  $4d$  electrons relative to the signal strength from the Cl  $3p$  electrons in going from UPS to XPS data. This effect is due to the strong dependence of the valence-band photoionization cross sections with the increase of the photon energy.<sup>17</sup> The comparison with the  $\text{RuO}_2$  PE spectrum shows that in this compound the  $4d^4$  final-state structure is displaced from a Fermi energy of about 0.6 eV. The experimental density of states is in good agreement with the theoretical density-of-states curves.<sup>24,27</sup> The calculated DOS curves<sup>20</sup> show that the metal-oxygen covalency-overlap interactions determine the width of the valence and conduction bands. In particular, most of the  $4d$  bandwidth arises from the overlap interactions of the  $t_{2g}$  and  $e_g$  orbitals with the oxygen  $2s$ - $2p$  states; the Fermi level falls at the lower part of the  $4d$  band, in the  $t_{2g}$  manifold. Thus the Ru  $4d$  states broaden into a dispersive, partly filled band, where metallic conduction is possible. The electron transport properties are then explainable in terms of normal behavior, as described by the Boltzmann equation.<sup>28</sup> In metallic  $\text{RuO}_2$  the screening in the final state is more effective than in nonmetallic  $\text{RuCl}_3$ , therefore it is not surprising that the peak in the  $4d^4$  structure in  $\text{RuCl}_3$  is found around 1 eV (XPS) as compared to 0.6 eV in  $\text{RuO}_2$ . The entire Cl  $3p$  band exhibits a full width at half maximum (FWHM) of about 5 eV, while the Ru  $4d$  peak has a broadening of 1.5 eV in XPS and 1.0 eV in UPS spectra. The dominant source of the linewidth in  $d$  levels is most probably hybridization broadening; that is, the effect of hybridizing the  $4d$  hole orbitals with anion  $3p$  orbitals, whose energies are spread over a considerable bandwidth (about 5 eV according to Fig.

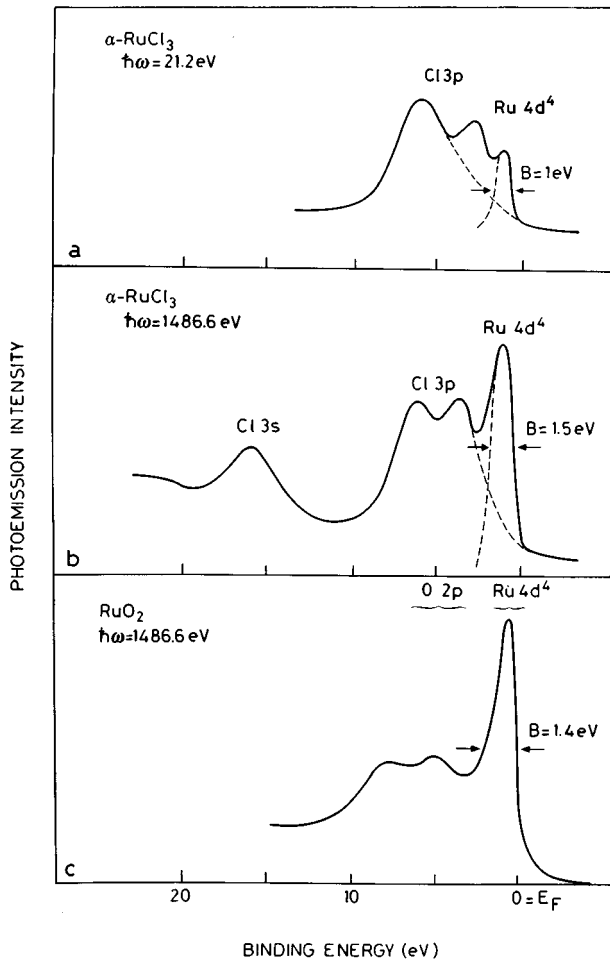


FIG. 1. Valence-band structure of paramagnetic  $\alpha$ - $\text{RuCl}_3$ : (a) Angle-resolved photoemission spectrum measured at normal emission with a He I radiation. (b) Angle-integrated photoemission spectra measured with Al  $K\alpha$  radiation. (c) XPS spectrum of metallic  $\text{RuO}_2$  (Ref. 21). The Fermi level is to be identified with zero binding energy.

1). In the case of the  $4d$  structure observed in UPS/XPS spectra, one observes a considerable broadening (1–1.5 eV), for the bandwidth of the  $t_{2g}$  orbitals (Frenkel excitons) of the  $4d^4$  ligand-field state  ${}^3T_1$ , while typical widths of ligand-field transitions in the optical spectrum are of the order of 0.1–0.2 eV. Since we are considering the same  $d$  states, it is not at once evident why the hopping of  $4d$  electrons between neighboring cations should produce widths much larger than the exciton widths (0.1–0.2 eV). The reason is that an exciton transfer consists of the excited electron hopping simultaneously with the hole from which it was excited. The effective exciton transfer integrals are of the order of  $2t^2/U$  (in the AF phase, but also above  $T_N$  where short-range order still occurs) rather than  $t$ , a typical  $d$ -hopping integral. For instance, in NiO or CoO the effective  $3d$ -transfer integral is of the order of  $10^{-3}$  eV, which corresponds to an intrinsic bandwidth of the order of  $10^{-2}$  eV, far smaller than the observed exciton widths (about 0.1 eV). In the case of the  $4d$  structure observed in UPS/XPS, there is no such extra particle-hole factor  $2t/U$  to reduce the hopping contribution to the widths of the final  $4d$  state in  $\text{RuCl}_3$ : one therefore

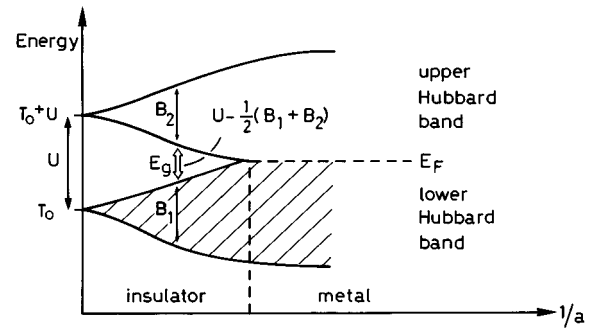


FIG. 2. Mott-Hubbard energy-level diagram for an unfilled  $d$  band in a solid as a function of the inverse lattice parameter. The separation at  $1/a=0$  is  $U$ , the Coulomb repulsion between two electrons of opposite spins simultaneously located in Wannier states centered on the same ion core. The two energy levels broaden with increasing  $1/a$ , and their separation is the energy gap  $E_g$ , the activation energy for conduction. In the zero bandwidth limit, the Bloch energies  $T_0$  are separated by  $U$ .

observes a greater broadening (width 1–1.5 eV) of the partial bandwidth due to  $t_{2g}$  and  $e_g$  orbitals, arising from the effective  $d$ - $d$  hopping integrals.<sup>2,14</sup>

The energy gap, ascribed to  $d$ - $d$  transitions, is

$$E_G = U - \frac{1}{2}(B_1 + B_2), \quad (2)$$

where  $U$  is the (atomic) Coulomb correlation energy, and  $B_1$  and  $B_2$  are the widths of the two bands. In Fig. 2 a Mott-Hubbard energy-level diagram for an unfilled  $d$  band in a solid is illustrated. We see that the separation at  $1/a=0$  is

$$U = I - EA; \quad (3)$$

that is, for many electron atoms  $U$  is defined as the energy required to transfer an electron from one atom to another, so that  $U$  is given by the ionization energy ( $I$ ) minus the electron affinity ( $EA$ ). With increasing  $1/a$  the two energy levels are broadened by ion-ion interaction in the solid, and their separation is the gap energy given by Eq. (2). It is seen that for a vanishingly small bandwidth, the band  $d$  splits into two subbands (upper and lower Hubbard bands) separated by an energy gap  $E_G$  of the order of  $U$ . Hubbard<sup>15</sup> in an approximate solution found that ordinary band theory predicted correct electrical behavior in the range where the ratio of the bandwidths  $B$  to  $U$  was large, but that near the opposite limit, when  $B \ll U$ , the material was indeed a Mott insulator: in the Hubbard approximation the Mott transition comes at  $B/U \sim 1.16$  (the dashed line in Fig. 2). A typical example is NiO, which for a long time was considered a prototype of a Mott insulator. Since for  $\text{Ni}^{2+}$  the atomic limit is  $U = 18$  eV (Ref. 29) and  $W \approx 1-3$  eV,<sup>30</sup> even with a considerable reduction of  $U$  by solid-state screening the insulating nature of NiO is understandable in this simple picture.

A central element in Hubbard's treatment of correlation effects and in any discussion of conduction mechanisms in narrow-band materials is the  $d$ -state bandwidth. For  $\alpha$ - $\text{RuCl}_3$ , one finds from PES spectra that the bandwidth is of the order of 1–1.5 eV in line with the reported widths of TMO's (Ref. 17) and TMH's.<sup>30</sup> In particular, from UPS spectra one can make an estimation of the Ru

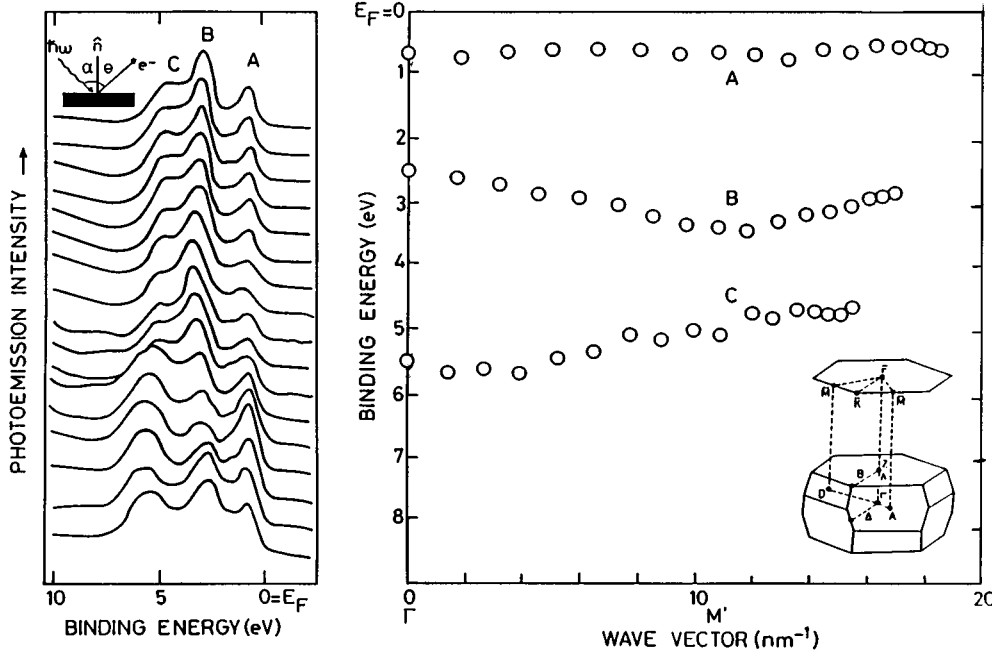


FIG. 3. Polar spectra of  $\alpha$ - $\text{RuCl}_3$  measured at 300 K.  $\alpha_i=45^\circ$  is the photon incidence angle, and  $\theta$  is the polar angle. The azimuthal angle corresponds to the  $\Gamma M' \Gamma$  direction of the surface Brillouin zone. The experimental band structure  $E$  vs  $k_{\parallel}$  in the repeated zone scheme for the  $\Gamma$ - $M'$ - $\Gamma$  symmetry direction is shown. In the insets the experimental geometry and the surface and bulk Brillouin zones for the  $\text{CdCl}_2$  structure are also shown.

$4d$ -bandwidth  $B$  of 0.7–0.8-eV FWHM for the  $^3T_1$  final state. In XPS spectra,  $B$  may be estimated at around 1.3–1.4 eV after correction for instrumental resolution. The photoconductivity edge, which gives the experimental value of the photoconductivity gap of the material (an energy separation between the  $d^4$  and  $d^6$  configurations) in a direct way, can be estimated around 0.7–0.8 eV (see Fig. 8 of Ref. 16). From Eq. (2) one thus obtains a value of  $U$  of 1.4–1.6 eV, which may be slightly reduced, if one makes a proper correction for hybridization, to  $1.2 \leq U \leq 1.4$  eV, but it still greater than the observed  $4d$ -band-width. Moreover, if one compares the obtained value of  $U$ , let us say  $U \sim 1.2$  eV, or a still lower value, like  $U \sim 0.8$ –1 eV (the value of the photoconductivity edge), with the dispersive part of the  $4d$  band (in Figs. 3 and 4), one finds that  $U$  is greater than five times the bandwidth of 0.2 eV (see Refs. 4 and 6). In the MH model a

nonmetallic behavior is thus expected, without considering a conventional band gap, and  $\alpha$ - $\text{RuCl}_3$  can be described as a Mott compound.<sup>16</sup>

Let us now present an angle-resolved photoemission investigation of the valence bands of  $\text{RuCl}_3$ . Figures 3 and 4 present angle-resolved spectra for the  $\Gamma M'$  and  $\Gamma K$  directions with energy relative to  $E_F$ , the Fermi level, and normalized photoemission intensity. The peak positions have then been plotted with the initial energy origin taken at  $E_F$  for the  $\Gamma M'$  and  $\Gamma K$  directions as a function of the wave vector  $k_{\parallel}$  by means of (1). The experimental plots  $E(k_{\parallel})$  along the  $\Gamma M'$  and  $\Gamma K$  orientations are also shown in Figs. 3 and 4, respectively. One can see that the experimental band structure extends across the first BZ, entering the second BZ along the  $\Gamma K$  and  $\Gamma M'$  symmetry lines.

Three prominent features have been identified and labeled

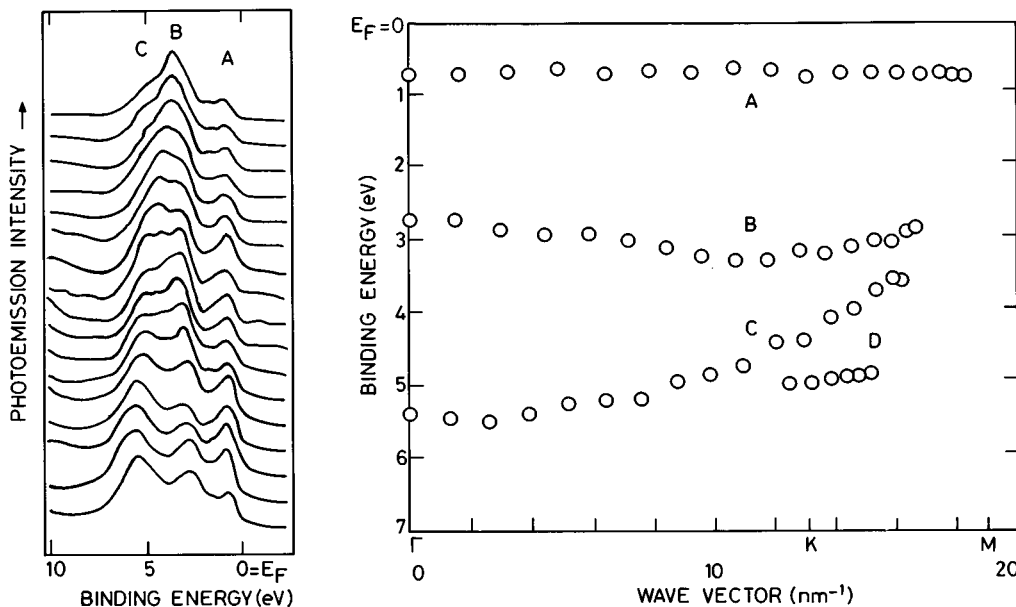


FIG. 4. Polar spectra of  $\alpha$ - $\text{RuCl}_3$  at  $T \sim 300$  K with  $\alpha_i=45^\circ$ . The azimuthal angle was now chosen to correspond to the  $\Gamma K M$  direction of the surface Brillouin zone. The experimental band structure  $E$  vs  $k_{\parallel}$  in the repeated zone scheme for the  $\Gamma$ - $K$ - $M$  symmetry direction is shown.

as *A*, *B*, and *C*. The intensity of peak *A* is weaker than that of peaks *B* and *C*, in contrast to what is observed in XPS and, for this reason, peak *A* is attributed to the *d* states of Ru atoms. The second and third peaks (*B* and *C*) arise from the *3p* states of chlorine. The first *p* band (*B*) shows a clear dispersion which is not attenuated at high angles. Along  $\Gamma M'$  (Fig. 3), the *B* band is symmetrical with respect to the  $M'$  point, and reaches the  $\Gamma$  point of the second BZ at high angles. The second *p* band (*C*), which also has dispersion, does not follow the symmetry of the BZ. The extrapolation at constant binding energy of the *C* band along  $\Gamma K$  reaches point *M* at an energy near 6 eV, corresponding to the binding energy at the  $M'$  point (Fig. 4).

Feature *A*, about 0.75 eV below the Fermi level, shows a very weak dispersion, less than 0.2 eV across the entire Brillouin zone. We think that this dispersionless band near  $E_F$ , observed by a surface-sensitive technique, is a true feature of bulk  $\text{RuCl}_3$ . It is possible that the observed localization only occurs for Ru *4d* electrons at the surface; however, for a surface state we expect appreciable changes with photon energy or a contaminated surface, which we did not observe. One can learn many interesting things from the results presented in Figs. 3 and 4. First of all, they show that the fundamental difference between Ru *4d* and Cl *3p* lies in their energy bandwidths. The bandwidth for the chlorine bands is about 2 eV, while that of the Ru *4d* band is about 0.2 eV. For the *4d* band we obtain a ratio  $U/W_d \geq 7$ : this ratio, greater than unity, seems to indicate that the one-electron picture should not give a proper description of the *d* states (see, for example, the band calculation for *3d* bands in Cr and Ni halides made in Ref. 7), and that a more localized model would be a more appropriate approach.<sup>22</sup>

We interpret these results by assuming that the broad Cl *3p* bands provide enough of a degree of freedom for relaxation so that the PES experiment measures approximately the one-electron band structure. On the other hand, the localized *4d* band which has stronger correlations, cannot relax during the measurement, and therefore the final states are excited states, which can be assigned to  $4d^4$  unscreened holes. The narrowing of the dispersive part of the Ru *4d* band is thus believed to be due to *d*-level correlation effects. If this description of the electronic properties of  $\alpha\text{-RuCl}_3$  is valid, it also appears that the material investigated here does not seem to be a conventional band-gap semiconductor.

Thus, coming back to Fig. 1, where the comparison of the XPS valence-band spectrum of  $\alpha\text{-RuCl}_3$  with that of metallic  $\text{RuO}_2$  is shown, one can say that, although the XPS spectrum of  $\text{RuCl}_3$  is very similar, the Fermi level is not inside the  $t_{2g}$  manifold and the compound is not a metal; in addition, the covalency-overlap interactions do not seem strong enough for the formation of itinerant (bandlike) *4d* states. This also seems to be confirmed by the results of ARP spectra, which show almost dispersionless Ru *4d* bands along important symmetry lines. These data suggest that the *4d* states remain quite localized, and that electronic conduction in the *4d* narrow band is not possible because of the presence of the correlation gap, which prevents the material from becoming metallic.

A last comment about the absence of photoemission satellites in the PES data also seems important. It is well known

that photoemission satellites, which are due to multielectron effects involving the transition metal *d* and ligand *p* states, have been observed in Ni oxides and halides,<sup>3,4</sup> and also in  $\text{CoO}$  (Ref. 22) and  $\text{MnO}$ .<sup>31</sup> In all cases resonant photoemission has suggested that the satellite bands observed in the valence-band photoemission spectra of these compounds are due to  $3d^{n-1}$  final states, and that the main emission features are due to ligand-to-*3d* charge-transfer final states. It was also pointed out<sup>31</sup> that the satellite peaks are generally observed in transition-metal compounds which cannot be described by ligand-field theory. As recalled, in the valence-band photoemission of  $\alpha\text{-RuCl}_3$  no satellite peak occurs, and only the *4d* main structure is observed. While the absence of satellites seems to support the idea that the PES spectra of this compounds can be interpreted within a ligand-field picture, it further indicates that exchange and correlation effects (which are observed in final excited states created by the photoexcitation of the one-electron wave functions of the initial states), as given by the value of *U*, should not be very strong in  $\alpha\text{-RuCl}_3$ : in fact we have obtained  $1.2 \leq U \leq 1.4$  eV, to be compared with  $6 \text{ eV} \leq U \leq 9 \text{ eV}$  in  $\text{NiO}$ .<sup>4,32</sup>

The final part of Sec. III concerns the discussion of the electrical and optical properties of this material, which is characterized by a narrow band in the vicinity of the Fermi energy. For such materials [e.g.,  $\text{CrCl}_3$ ,<sup>7</sup> Ni halides,<sup>4-6,9</sup> or  $\text{NiO}$  (Refs. 4 and 5)], both electronic correlation and the electron-phonon coupling (small polarons) should be considered explicitly.<sup>14,33-36</sup>

The electrical conductivity measured in the paramagnetic phase of  $\alpha\text{-RuCl}_3$ , shown in Fig. 2 of Ref. 18, shows a temperature dependence typical of a semiconductor ( $\rho_{\text{RT}} \sim 2 \times 10^3 \Omega \text{ cm}$ ) with an activation energy around 0.1 eV below 300 K, and about 0.5 eV above 400 K, for the crystallographic directions parallel and perpendicular to the *c* axis. The fact that deviations from linearity occur above 400 K indicates that the lower activation energy may not be due to an intrinsic process. It is also worthwhile noting that the thermal activation energy for conduction above 400 K corresponds to an energy gap of about 1 eV very close to the value obtained in photoconductivity.<sup>16</sup> Hall-effect measurements performed in the layers perpendicular to the *c* axis in the 180–320-K range have been also reported.<sup>21</sup> The sign of Hall coefficient indicates electron conduction in the temperature region studied: the temperature dependence of the Hall mobility  $\mu$  varies as  $T^{-2,3}$ , and its value is  $0.1 < \mu < 1 \text{ cm}^2 \text{ V s}^{-1}$ . The decrease of the electron mobility indicates, according to Ref. 21, that the electrons (holes) move in the conduction (valence) band, derived from the  $4d^5$  crystal-field split levels with bandwidths about 0.1–0.2 eV, and separately by an energy gap  $E_G \sim 0.3$  eV. As a matter of fact, crystal-field excitations between single-ion  $4d^5$  spectral levels appear as a discrete structure in the absorption spectrum<sup>18</sup> observed below the outset of the strong *3p-4d* absorption edge of the electrical dipole-allowed charge-transfer transitions observed around 4 eV (see Fig. 9 of Ref. 16).

The absorption coefficient is of the order of  $10^4\text{--}10^5 \text{ cm}^{-1}$  over 1 eV, where a photoconductivity tail is observed, while two small peaks at 0.3 and 0.5 eV are measured with absorption coefficients of the order of  $10^3 \text{ cm}^{-1}$ . The absorption observed in the range 0.1–3 eV has been assigned to ligand-field transitions in terms of the Tanabe-Sugano dia-

gram for the  $d^5$  configuration,<sup>8</sup> with a value of the crystal-field splitting parameter  $\Delta_{\text{CF}}=1.4\text{--}1.5$  eV for the low-spin configuration (see Table I). While the low-energy weak peaks at 0.28 and 0.53 eV have been assigned to spin-forbidden transitions ( ${}^2T_2\rightarrow{}^6A_1$  and  ${}^2T_1\rightarrow{}^4A_1$ ), the first strong absorption peak at the 1.18- and 2.08-eV bands have been attributed to spin-allowed transitions ( ${}^2T_2\rightarrow{}^2A_2$ ,  ${}^2T_1$  and  ${}^2T_2\rightarrow{}^2T_2$ ,  ${}^2A_1$ ).

Table I reports the high-low spin change of the crystal-field parameter for some typical  $3d$  and  $4d$  transition-metal compounds.<sup>18–20</sup> An increase results in the ratio  $\Delta_{\text{CF}}/B$  when one considers a low-spin compound in which one moves to the right on a Tanabe-Sugano diagram.<sup>8</sup> In such conditions, for four-, five-, six-, and seven-electron systems and octahedral coordination,  $4d$  and  $5d$  electrons no longer follow the Hund spin alignment with promotion to  $e_g$  states, and favor double occupation of the  $t_{2g}$  states. The absence of  $e_g$  electrons in  $\text{RuCl}_3$  gives a value of  $\Delta_{\text{CF}}$  below that of  $\text{FeCl}_3$ , though the  $\Delta_{\text{CF}}/B$  ratio still remains larger in the  $4d$  compound.<sup>18</sup>

However, crystal-field excitations between localized states involve no transport of charge and should not contribute to electrical conductivity. As previously recalled, electrons are essentially localized in the narrow  $t_{2g}$  band (a bandwidth of about 0.2–0.3 eV) and cannot move, even if the band is not full, for the energy cost of transferring a  $4d$  electron to an adjacent site. The transport properties of the material<sup>18,21</sup> thus seem in contrast with the recent classification of  $\text{RuCl}_3$  as a MH insulator, based on PES results: that is, is  $\alpha\text{-RuCl}_3$  a band or Mott semiconductor?

If we accept a localized description of the valence-band  $d$  electrons, there is little reason to expect that the  $3d$ -electron wave vector be conserved in the photoemission process; hence the Ru  $4d$  profile in ARP spectra is expected to be unchanged with the electron wave vector, and just vary in intensity following the photoemission cross section. The experimental bandwidth of feature *A* assigned to Ru  $4d$  states show a very small dispersion ( $\leq 0.2$  eV), less than the one-electron bands. If the narrowing of the cation  $4d$  band can be considered a result of the  $d$ -level correlation effect, then we are left with a MH insulator, and it is not easy to explain its semiconductivity in the case of a pure, stoichiometric material.

On the other hand, one may consider that the weak dispersion of feature *A* observed in the photoemission spectra can be due to a small hybridization with ligand  $3p$  orbitals, which can delocalize the  $4d$  states to some extent, thereby making them describable within the band picture (different from the result of the ground-state calculations). Thus the weak dispersion of the Ru  $4d$  structure could have this origin, no different from the (stronger) dispersion effect observed in the  $3d$  band of  $\text{NiI}_2$ .<sup>37</sup> In the latter compound, a charge-transfer semiconductor, the observed transport process is then explained by hole conduction in the ligand I  $5p$  band,<sup>9,37</sup> and by polaronic conduction in the  $3d$  band.<sup>14</sup> Thus, if one insists in explaining the electrical properties of  $\text{RuCl}_3$  by means of a band picture model, one must claim that the partially hybridized  $4d$  states are not to be too localized, and that either carrier (electrons and holes) is moving in these states of large effective mass and with very low Hall mobility. The Hall measurement then specifies that the ma-

jority carriers are electrons.<sup>21</sup> This picture, which does not seem unreasonable, seems to indicate a smaller screening of the intra-atomic Coulomb repulsion, and that the low-spin compound is approaching the delocalization boundary.<sup>38,39</sup> In this sense consideration of the electronic absorption in the energy region over 3 eV, reported in the reflectance spectrum of Fig. 11 of Ref. 16, seems interesting. The “extra” absorption, observed in reflectance, between the first 1-eV spin-allowed  $d$ - $d$  transition (which in this material may approach delocalization through a covalency relaxation mechanism) and the first parity-allowed charge-transfer  $p$ - $d$  transition around 4 eV, consists of broad bands of slightly higher extinction coefficients than the accompanying ligand-field type, overlapping to produce long, relatively unstructured absorption and a photoconductivity tail. The photocurrent, due to the excitation of electron-hole pairs in the MH bands, steadily increases up to 2.5–3 eV and is observed in the region where the extra absorption occurs. On decreasing correlation one must progressively move towards a one-electron band description, passing through a region where the two descriptions (ligand field vs one-electron band picture) must be merged. This extra absorption may thus be considered as an indication for delocalized  $d$ - $d$  ligand-field transitions rather than intersite hopping transitions, which seem to occur most likely in strongly hybridized, low-spin compounds.

Thus, although this magnetic material can be described by means of a localized model of the grounds of its spectroscopic, electronic, and magnetic features, the room-temperature transport properties, if they are not of extrinsic origin (tentatively ruled out by Refs. 18 and 21), seem to indicate a more conventional approach based on a band model. One should conclude that the theory of either photoemission or layered TMH’s (or both) is poorly understood. The implication is that one should be cautious in making deep interpretations when the general phenomenology is in part contradictory (i.e., inconsistency between photoemission results and transport properties) and incomplete. For a better understanding of these materials with open  $4d$  or  $5d$  shells, further investigations, both theoretically (band or localized model calculations) and experimentally (new transport measurements on pure, stoichiometric, carefully checked crystals, and perhaps resonant photoemission with a synchrotron source), seem necessary and are called for.

#### IV. CONCLUSIONS

A recent study of the electronic properties of the low-spin compound  $t_{2g}^5 \alpha\text{-RuCl}_3$  suggested that this material may be classified as a Mott-Hubbard insulator. This was not an evident result for a  $4d$  compound, since the larger  $d$  orbitals imply smaller correlation  $U$  and larger bandwidth  $B$  parameters, weakening the Mott tendency for many  $4d$  and  $5d$  cations. The less corelike nature of the  $4d$  orbitals, manifested in more hybridization, is evidenced by a larger crystal-field parameter  $\Delta_{\text{CF}}\approx 1.5$  eV and smaller Racah parameter ( $B=370$  cm<sup>-1</sup>), due to both larger average radii and increased covalency.

Photoelectron spectroscopy has been used in order to determine the energy separation of the localized Ru  $4d$  states from the Cl  $3p$  bands, and their dispersion curves in the Brillouin zone. Angle-integrated and -resolved photoemis-

sion, together with photoconductivity, give an estimation of the Coulomb correlation energy  $U = 1.4\text{--}1.6$  eV. It is found that the Ru  $4d$  states, separated by 2 eV from the top of the valence-band  $3p$  states, do not disperse more than  $\pm 0.1$  eV across the entire Brillouin zone. It is believed that the observed lack of dispersion is evidence of localized  $4d$  electrons. In line with a Mott-Hubbard model, valid for  $U/W_d > 1$ , it is found that the estimated ratio for  $\alpha\text{-RuCl}_3$  is  $\geq 7$  and, therefore, it is believed that a localized picture may be a more appropriate approach for the description of its electronic, optical, and magnetic properties.

However, this description seems contradictory with the transport properties describing the material as a conventional band-gap semiconductor. In addition, one-electron band calculations are not known for  $\alpha\text{-RuCl}_3$ , and from a comparison with the XPS spectrum of  $\text{RuO}_2$ , which is bandlike, one cannot rule out *a priori* a standard band picture for  $4d$  states owing to the strong similarity of the spectra. Thus, although one cannot exclude a band conduction for the description of the electrical properties of this compound approaching the delocalization boundary, in consideration of its optical and magnetic characteristics and angle-resolved photoemission

results one can also regard it as an unconventional semiconductor<sup>39</sup> in the Mott sense. The apparent inconsistency between photoemission and transport results may be understood by considering that photoemission investigates the multielectron excited-state system under relaxation corrections greater than the relevant bandwidth ( $4d$  band), while transport measurements study the ground-state behavior of the system. In photoelectron spectra of Mott materials the multiplet structure of  $d$  states is observed, which is characteristic of the final-state electron count, not the initial state.<sup>17,32</sup> In conclusion we suggest that for  $\alpha\text{-RuCl}_3$  the appellation ‘‘Mott insulator’’ is more informative in regard to the transport and magnetic characteristics of this material than the label of ‘‘band-gap semiconductor’’ attributed to it in the literature.

#### ACKNOWLEDGMENTS

The photoemission measurements have been performed at the University of Toulouse, Solid State Physics Laboratory, as a part of an international cooperation research program. I thank B. Carricaburu and R. Mamy for experimental work and critical comments on the whole subject.

- 
- <sup>1</sup>D. Adler, in *Solid State Physics*, edited by H. Ehrenreich and D. Turnbull (Academic, New York, 1968), Vol. 21, p. 1.
- <sup>2</sup>B. H. Brandow, *Adv. Phys.* **26**, 651 (1977).
- <sup>3</sup>A. Fujimori and F. Minami, *Phys. Rev. B* **30**, 957 (1984).
- <sup>4</sup>G. A. Sawatzky and J. W. Allen, *Phys. Rev. Lett.* **53**, 2339 (1984).
- <sup>5</sup>K. Terakura, A. R. Williams, T. Oguchi, and J. Kübler, *Phys. Rev. Lett.* **52**, 1830 (1984).
- <sup>6</sup>K. Terakura, A. R. Williams, T. Oguchi, and J. Kübler, *Phys. Rev. B* **30**, 4734 (1984).
- <sup>7</sup>S. Antoci and L. Mihich, *Phys. Rev. B* **18**, 5768 (1978); **21**, 3383 (1980).
- <sup>8</sup>S. Sugano, Y. Tanabe, and H. Kamimura, *Multiplets of Transition-Metal Ions in Crystals* (Academic, New York, 1970).
- <sup>9</sup>C. R. Ronda, G. J. Arends, and C. Haas, *Phys. Rev. B* **35**, 4038 (1987).
- <sup>10</sup>O. K. Andersen, H. L. Skriver, H. Hohl, and B. Johansson, *Pure Appl. Chem.* **52**, 93 (1979).
- <sup>11</sup>T. Oguchi, K. Terakura, and A. R. Williams, *Phys. Rev. B* **28**, 6443 (1983).
- <sup>12</sup>A. Svane, *Phys. Rev. Lett.* **68**, 1900 (1992).
- <sup>13</sup>N. F. Mott, *Proc. Phys. Soc. London Sect. A* **62**, 416 (1949).
- <sup>14</sup>N. F. Mott, *Metal-Insulator Transitions*, 2nd ed. (Taylor & Francis, London, 1990).
- <sup>15</sup>J. Hubbard, *Proc. R. Soc. London Ser. A* **276**, 238 (1963); **277**, 237 (1964); **281**, 401 (1964).
- <sup>16</sup>I. Pollini, *Phys. Rev. B* **50**, 2095 (1994), and references therein.
- <sup>17</sup>D. E. Eastman and J. L. Freeouf, *Phys. Rev. Lett.* **34**, 395 (1975).
- <sup>18</sup>L. Binotto, I. Pollini, and G. Spinolo, *Phys. Status Solidi B* **44**, 245 (1971).
- <sup>19</sup>I. Pollini and G. Spinolo, *Phys. Status Solidi* **41**, 691 (1970).
- <sup>20</sup>J. A. Wilson, *Adv. Phys.* **21**, 143 (1972).
- <sup>21</sup>S. Rojas and G. Spinolo, *Solid State Commun.* **48**, 349 (1983).
- <sup>22</sup>N. B. Brooks, D. S. Law, D. R. Warburton, P. L. Wincott, and G. Thornton, *J. Phys. Condens. Matter* **1**, 4267 (1989); Z. X. Shen, J. W. Allen, P. A. Lindberg, D. S. Dessau, B. O. Wells, A. Borg, W. Ellis, J. S. Kang, S. J. Oh, I. Lindau, and W. E. Spicer, *Phys. Rev. B* **42**, 1817 (1990).
- <sup>23</sup>P. B. Allen and N. Chetty, *Phys. Rev. B* **50**, 14 855 (1994).
- <sup>24</sup>L. F. Mattheis, *Phys. Rev. B* **13**, 2433 (1976).
- <sup>25</sup>J. Riga, C. Tenet-Noël, J. J. Pireaux, R. Caudano, J. J. Verbist, and Y. Gobillon, *Phys. Scr.* **16**, 351 (1977).
- <sup>26</sup>R. R. Daniels, G. Margaritondo, C. A. Georg, and F. Levy, *Phys. Rev. B* **29**, 1813 (1984).
- <sup>27</sup>J. H. Xu, J. Jarborg, and A. J. Freeman, *Phys. Rev. B* **40**, 7939 (1989).
- <sup>28</sup>K. M. Glassford and T. R. Chelikowsky, *Phys. Rev. B* **49**, 7107 (1994).
- <sup>29</sup>C. E. Moore, *Atomic Energy Levels*, Natl. Bur. Stand. (U.S.) Circ. No. 35 (U.S. GPO, Washington, D.C., 1971), Vol. 1.
- <sup>30</sup>S. Hüfner and G. K. Wertheim, *Phys. Rev. B* **8**, 4857 (1973).
- <sup>31</sup>R. J. Lad and V. E. Heinrich, *Phys. Rev. B* **38**, 10 860 (1988).
- <sup>32</sup>S. Hüfner, *Photoelectron Spectroscopy*, Solid State Science Vol. 32 (Springer-Verlag, Berlin, 1995).
- <sup>33</sup>F. Holstein, *Ann. Phys.* **8**, 343 (1959).
- <sup>34</sup>Ya. M. Ksendzov, L. N. Ansel'm, L. L. Vasileva, and V. M. Latysheva, *Fiz. Tverd. Tela (Leningrad)* **5**, 1537 (1963) [*Sov. Phys. Solid State* **5**, 1116 (1963)].
- <sup>35</sup>V. P. Shuze and A. Z. Shelykh, *Fiz. Tverd. Tela (Leningrad)* **5**, 1756 (1963) [*Sov. Phys. Solid State* **5**, 1278 (1963)].
- <sup>36</sup>J. Feinleib and D. Adler, *Phys. Rev. Lett.* **21**, 1010 (1968).
- <sup>37</sup>H. I. Starnberg, M. T. Johnson, and H. P. Hughes, *J. Phys. C* **19**, 2689 (1986).
- <sup>38</sup>C. H. Maule, J. N. Tothill, P. Strange, and J. A. Wilson, *J. Phys. C* **21**, 2153 (1988).
- <sup>39</sup>J. A. Wilson, in *The Metallic and Nonmetallic States of Matter*, edited by P. P. Edwards and C. N. Rao (Taylor & Francis, London, 1985), pp. 215–260.